

Research Paper

Contributions of subolemmal acidic vesicles and microvilli to the intracellular Ca^{2+} increase in the sea urchin eggs at fertilization

F. Vasilev^{1,✉}, N. Limatola², J.T. Chun¹, L. Santella²

1. Department of Biology and Evolution of Marine Organisms, Stazione Zoologica Anton Dohrn, Napoli, Italy

2. Department of Research Infrastructures for Marine Biological Resources, Stazione Zoologica Anton Dohrn, Napoli, Italy

✉ Corresponding author: Filip Vasilev, Ph.D. Phone: +39 081-583-3407; Fax: +39 081-583-3289; Email: filip.vasilev@szn.it

© Ivyspring International Publisher. This is an open access article distributed under the terms of the Creative Commons Attribution (CC BY-NC) license (<https://creativecommons.org/licenses/by-nc/4.0/>). See <http://ivyspring.com/terms> for full terms and conditions.

Received: 2018.07.11; Accepted: 2018.12.15; Published: 2019.01.29

Abstract

The onset of fertilization in echinoderms is characterized by instantaneous increase of Ca^{2+} in the egg cortex, which is called 'cortical flash', and the subsequent Ca^{2+} wave. While the cortical flash is due to the ion influx through L-type Ca^{2+} channels in starfish eggs, its amplitude was shown to be affected by the integrity of the egg cortex. Here, we investigated the contribution of cortical granules (CG) and yolk granules (YG) to the sperm-induced Ca^{2+} signals in sea urchin eggs. To this end, prior to fertilization, *Paracentrotus lividus* eggs were treated with agents that disrupt or relocate CG beneath the plasma membrane: namely, glycyl-L-phenylalanine 2-naphthylamide (GPN), procaine, urethane, and NH_4Cl . All these pretreatments consistently suppressed the cortical flash in the fertilized eggs, and accelerated the decay kinetics of the subsiding Ca^{2+} wave in most cases. By contrast, centrifugation of the eggs, which stratifies organelles but not the CG, did not exhibit such changes except that the CF was much enhanced in the centrifugal pole where YG are localized. Surprisingly, we noted that pretreatment of the eggs with these CG-disrupting agents or with the inhibitors of L-type Ca^{2+} channels all drastically reduced the density of the microvilli and their individual shapes on the egg surface. Taken together, our results suggest that the integrity of the egg cortex ensures successful generation of the Ca^{2+} responses at fertilization, and that modulation of microvilli shape and density may serve as a mechanism of controlling ion flux across the plasma membrane.

Key words: cortical flash, cortical granules, microvilli, fertilization, calcium, actin

1. Introduction

At fertilization, eggs of all animal species display an increase of intracellular Ca^{2+} , which is used as a biochemical signal to activate the egg. Historically, starfish and sea urchin eggs have been used as suitable experimental models for studying the universal phenomenon of the Ca^{2+} signaling in fertilized eggs in which the sperm-triggered Ca^{2+} increase resumes the meiotic cycle, induces protein and DNA synthesis, and initiates the embryonic development.

The sperm-induced Ca^{2+} increase in the fertilized egg is mainly due to the ion influx and to the release from internal Ca^{2+} stores, e.g. the endoplasmic

reticulum (ER) and acidic vesicles. In sea urchin eggs, the intracellular Ca^{2+} increase takes place in two sequential events. First, upon the sperm-egg fusion, the egg membrane potential depolarizes and the L-type Ca^{2+} channels open (influx). This leads to a synchronized Ca^{2+} increase in the entire subplasmalemmal region, which is known as 'cortical flash' (CF). The electrical change of the plasma membrane induced by the fertilizing sperm is thought to render the fertilized egg refractory to the entry of additional spermatozoa: the fast electrical block to polyspermy [1]. The CF, which lasts about 13.5 sec in sea urchin eggs, precedes the onset of the Ca^{2+} wave

[2]. Thus, the rise of the Ca^{2+} wave appears to require a latent period, which can be defined here as the time lag from the beginning of the CF to the onset of the Ca^{2+} wave that starts from the sperm-egg interaction site. The Ca^{2+} wave then propagates to the antipode, triggering CG exocytosis. As a result, the vitelline layer elevates to form the fertilization envelope (FE), which has been suggested as a mechanism of mechanical block to polyspermy [3,4].

A few second messengers can mobilize intracellular Ca^{2+} in sea urchin eggs, mimicking the Ca^{2+} wave in fertilized eggs. Inositol 1,4,5-trisphosphate (InsP_3) and cyclic ADP-ribose (cADPr) open the cognate InsP_3 and ryanodine receptors on the ER, respectively. On the other hand, nicotinic acid adenine dinucleotide (NAADP) may liberate Ca^{2+} from distinct internal stores such as reserve (yolk) granules, the lysosome-related vesicles in sea urchin eggs [5,6].

The cortex of echinoderm eggs, through which the sperm-induced Ca^{2+} signals originate and propagate, consists of the ER, and CG which are interconnected and attached to the plasma membrane by a meshwork of F-actin [7]. The egg surface, where Ca^{2+} influx takes place, is covered with microvilli filled with actin filaments that undergo constant treadmilling [8,9]. The tip of the microvilli may assist in recognizing the sperm by means of cognate receptors [10,11]. Hence, the actin filaments in the microvilli and in the subplasmalemmal region may have profound impacts on sperm-egg recognition and binding, as well as on the subsequent signal transduction. In sea urchin eggs, the sperm-fusion site forms a fertilization cone made of F-actin, and this structure is thought to be instrumental in engulfing the sperm [12]. In echinoderm, in parallel with the Ca^{2+} increases and CG exocytosis, fertilized eggs exhibit microvilli elongation into the perivitelline space. Emanating from the egg surface to connect to the FE, the extending microvilli and spikes containing F-actin may provide equidistant separation of the vitelline layer or accommodate the excessive plasma membrane that was produced as a result of the CG exocytosis and membrane fusion [13,9]. The structural modification in the maturing oocytes of starfish might also underlie the changes of the electrical properties of the plasma membrane [14,15]. In line with that, deprivation of external Ca^{2+} during meiotic maturation, which caused significant changes in the cortical region of the oocytes in terms of the positioning of the vesicles, microvillar morphology and the thickness of the F-actin layer, also resulted in much reduced Ca^{2+} influx when the eggs were fertilized in the artificial seawater containing Ca^{2+} [16]. This finding may be ascribed to the fact that ion

channels and pumps are often associated with the neighboring actin filaments that may modulate their activity [17-19].

Sea urchin eggs contain various types of acidic vesicles with different functions and capacity to store Ca^{2+} . CG in a typical sea urchin egg are over 15,000 in number [20]. They are normally docked to the plasma membrane and contain enzymes that contribute to the formation of the FE matrix. Besides serving as a calcium store, CG may synthesize Ca^{2+} -linked second messengers, as two isoforms of ADP-ribosyl cyclase (ARC) are located in their lumen to generate cADPr in a pH-dependent manner [21]. Another class of vesicles are so-called 'white' or 'clear' vesicles (acidocalcisomes), representing acidic calcium-storage compartments with high content of polyphosphates (poly P). These vesicles, which translocate towards the centripetal part after egg centrifugation [22], are not sensitive to the lysosome-disrupting GPN, and their Ca^{2+} is released by poly P hydrolysis, but not by NAADP [23]. Perhaps the largest and most abundant acidic vesicles are the YG that comprise one third of the total cell volume [24] and provide nutrients for the developing embryo [25]. The presence of the lysosome-related proteins in the lumen of the YG makes them a part of the endo-lysosomal system, as they are probably derived from the endosomes acquired during oogenesis [26,27]. Despite the mild acidic pH (6.8), YG are easily stained with Acridine orange and LysoTracker-RED DND99 [22,28] and tend to shift to the centrifugal pole when the egg is stratified by centrifugation [29]. Consistent with the high Ca^{2+} content in the lumen, these vesicles were implicated in NAADP-sensitive Ca^{2+} release through two-pore channels (TPCc) [5]. Finally, being located near CG, there are pigment granules with unknown concentration of Ca^{2+} . These granules are 1 μm in diameter and low in number. As with clear vesicles, the pigment granules tend to shift to the centripetal pole in the stratified egg [20,30].

Acidic vesicles represent a non-ER Ca^{2+} store that contributes to the Ca^{2+} increase in the sea urchin egg in response to NAADP photoactivation [29,6]. In starfish eggs, photoactivation of caged NAADP induces depolarization of the membrane potential and the Ca^{2+} influx which is completely inhibited when NAADP uncaging is performed in CaFSW [31-34]. Both membrane current and the CF are severely reduced when the subplasmalemmal actin cytoskeleton was altered prior to fertilization or NAADP uncaging [35]. One intriguing unsolved question regarding NAADP is that it appears to stimulate Ca^{2+} transport across the plasma membrane in starfish eggs [35,36], whereas the same second

messenger can induce a CF in sea urchin eggs mainly from the internal stores such as acidic vesicles [37]. However, during sea urchin fertilization in artificial seawater containing low Ca^{2+} concentration (1 mM), the sperm-initiated CF is substantially reduced [2], as opposed to when the caged NAADP is photoliberated [38]. This observation casts a doubt on the role of NAADP in generating the Ca^{2+} influx in the fertilized eggs of sea urchin [39]. Nonetheless, it is the NAADP-triggered Ca^{2+} increase that resembled the CF most, while the InsP_3 - and cADPr-sensitive Ca^{2+} stores in sea urchin eggs may be interconnected to the NAADP-sensitive Ca^{2+} stores [6,37]. Thus, in view of the contradicting data on how acidic vesicles may contribute to the CF at fertilization of sea urchin eggs [32,39], we examined the effect of their depletion on Ca^{2+} signaling at fertilization. We previously reported that a brief preincubation of starfish eggs with the Ca^{2+} ionophore ionomycin, which caused interfusion of CG and white vesicles, led to significant suppression of CF at fertilization [40]. These results suggested that these vesicles may be somehow linked to CF [41,21]. One conceivable model in this regard is a morpho-functional interplay between the Ca^{2+} channels in the plasma membrane and the acidic vesicles nearby, which may serve as an internal Ca^{2+} store. In the present study, we tested this idea by inducing structural changes to the CG and vesicles in the tight subplasmalemmal zone of sea urchin eggs prior to fertilization. Firstly, we used GPN to induce rupture or interfusion of CG and vesicles. Secondly, we tested the effect of weak base NH_4Cl and the anesthetics like urethane and procaine on the CF and Ca^{2+} waves in fertilized eggs. The pretreatment with these agents was known to block CG exocytosis in the fertilized eggs of sea urchin by dislocating the granules and vesicles towards the inner cytoplasm [42-45]. Finally, we stratified the eggs by centrifugation so as to only dislodge the vesicles and organelles from their original subcellular location, and not the CG. Being tightly attached to plasma membrane, most CG remain near the plasma membrane, whereas only the YG migrate towards the centrifugal egg pole, and the ER and the nucleus to the opposite centripetal side [22,29,30]. By examining the sea urchin egg surface topography and the ultrastructural modifications of the subplasmalemmal regions in relation to their effects on the CF and Ca^{2+} waves at fertilization, we drew the conclusion that the natural distribution of microvilli and the correct positioning of CG in the vicinity of the plasma membrane are required for the proper occurrence of sperm-induced Ca^{2+} signals.

2. Materials and methods

2.1. Preparation of gametes.

Paracentrotus lividus were collected from the Gulf of Naples during the breeding season from November to April and maintained in seawater at 16 °C. Eggs and sperm were collected by the intracoelomic injection of 0.5 M KCl. All experiments were performed in filtered seawater (FSW) except for certain experiments done in the artificial seawater (ASW: 575 mM NaCl, 10 mM KCl, 10 mM CaCl_2 , 44 mM MgSO_4 , 11 mM MgCl_2 , 2 mM NaHCO_3 , pH 8.2) and in the low Ca^{2+} ASW (575 mM NaCl, 10 mM KCl, 1 mM CaCl_2 , 44 mM MgSO_4 , 20 mM MgCl_2 , 2 mM NaHCO_3 , pH 8.2). Spermatozoa were prepared in FSW 1 minute before insemination to a final density of 3.5×10^{-6} per ml.

2.2. Confocal microscopy and Ca^{2+} measurement.

To stain lysosome-like acidic vesicles, *P. lividus* eggs were incubated in FSW containing 10 nM LysoTracker-RED DND 99 (Molecular Probes) for 1 h. To assess the effect of GPN, these eggs were subsequently exposed to either 200 μM GPN (Santa Cruz Biotechnology) or control 0.05 % dimethyl sulfoxide (DMSO) in seawater. The fluorescence changes in the stained vesicles were examined in the same eggs before and after 40 minutes incubation with GPN (or DMSO) by use of Zeiss LSM 510 META laser scanning confocal microscope (Jena, Germany). Some eggs were then fertilized, and the fluorescent images were captured 25 minutes later. To monitor the intracellular Ca^{2+} changes, a mix of calcium dye (Calcium Green) conjugated to 10 kDa dextran (Molecular Probes) and Rhodamine-Red (35 μM) was prepared in the injection buffer [9] and microinjected into *P. lividus* eggs by use of air-pressured microinjector (eppendorf FemtoJet). After each microinjection, eggs were left for 20 minutes in FSW before every treatment. Immobilized in a chamber, intact eggs were mounted on a Zeiss Axiovert 200 microscope with a Plan-Neofluar 20x/0.50 objective to monitor the cytosolic Ca^{2+} changes during fertilization with a cooled CCD camera (MicroMax, Princeton Instruments, Inc., Trenton, NJ). Quantification of the Ca^{2+} data was presented as a relative fluorescent unit (RFU) calculated from a given time point and normalized to the baseline fluorescence (F_0) following the formula $F_{\text{rel}} = [F - F_0] / F_0$, where F represents the average fluorescence level of the entire oocyte. All the Ca^{2+} data were analyzed with the MetaMorph Imaging System software (Universal Imaging Corporation, West Chester, PA).

2.3. Chemicals and pharmacological inhibitors.

Diltiazem and Verapamil were purchased from Sigma-Aldrich and dissolved in distilled water. Both inhibitors were used to incubate the eggs at the final concentration of 10, 50 and 100 μM for 40 minutes before spermatozoa were added. Urethane and procaine (Sigma-Aldrich) were dissolved in the FSW. Eggs exposed to 400 mM urethane for 5 minutes were transferred to FSW and incubated for 5 minutes before insemination. In the case of procaine (10 mM final concentration), eggs were treated for 20 minutes and then transferred to FSW and immediately inseminated. The treatment with the NH_4Cl was for 30 minutes at the final concentration of 40 mM (pH 9.0), after which the eggs were transferred to FSW and then fertilized.

2.4. Egg stratification.

The procedure was adapted from Lee et al 2000 [29]. *P. lividus* eggs were microinjected with the calcium dye mix, incubated in FSW for 10 minutes and then centrifuged in FSW containing 1 % sucrose (dissolved in distilled water) for 30 minutes (12,000 g). After centrifugation, eggs were washed for 5-10 minutes in FSW to remove the sucrose and then inseminated.

2.5 Transmission and Scanning Electron Microscopy (TEM and SEM).

Sea urchin eggs were fixed in FSW containing 0.5 % glutaraldehyde for 1 hour. Samples were then post-fixed with 1 % osmium tetroxide and dehydrated in a series of ethanol solutions of increasing concentration. The embedded samples in EPON were polymerized for 2 days at 60°C in a dry oven. Ultrathin sections for TEM observation (ZEISS LEO 912 AB) were stained with UAR-EMS Uranyl acetate replacement staining and lead citrate. For SEM observation, ethanol-treated samples were further dehydrated by a critical point dryer (CPD300, Leica), and subsequently sputtered with gold and observed with a JEOL 6700F scanning electron microscope. For quantification, microvilli visualized in SEM were counted from three separate regions (26.1 μm^2) randomly selected from 4 different eggs for each experiment, and the results were analyzed with t-test and ANOVA by use of Prism 3.0.

3. Results

3.1. The cortical flash in the fertilized eggs of sea urchin is mainly derived from the external source.

To test if the CF depends on external Ca^{2+} , *P. lividus* eggs were fertilized in ASW containing 10 or 1

mM Ca^{2+} following 10 minutes preincubation. As sperm motility requires Ca^{2+} in the media, fertilization does not take place in Ca^{2+} -free seawater. In the 1 mM ASW, however, the time needed for the sperm to induce intracellular Ca^{2+} increases in the eggs was more than 5 fold longer (490.7 ± 385.5 sec, $n=19$) in comparison with the control eggs in ASW containing 10 mM Ca^{2+} (82.9 ± 129.9 sec, $n=23$; $P<0.0001$). As shown in (Fig 1A), lowering the Ca^{2+} concentration in the medium produced a significant decrease in the amplitude of the CF (0.02 ± 0.006 RFU, $n=5$) compared to the control eggs (0.09 ± 0.008 RFU, $n=9$; $P<0.001$), whereas the peak amplitude of the Ca^{2+} wave was not significantly changed (1 mM ASW, 0.66 ± 0.16 RFU; 10 mM ASW, 0.67 ± 0.14 RFU; $P=0.9423$). These data confirmed the reports from other species of sea urchin [2]. Thus, unlike the Ca^{2+} wave, the synchronized Ca^{2+} increase taking place in the entire egg surface for the initial 10 seconds of fertilization was heavily dependent upon external Ca^{2+} . To further examine if the voltage-gated calcium channels are involved in the generation of the CF, we fertilized sea urchin eggs pretreated with 10, 50 and 100 μM L-type Ca^{2+} channels inhibitors diltiazem and verapamil. Both inhibitors caused significant suppression of the CF in a dose-dependent manner (Fig. 1D, red lines) until the higher doses of the drugs also modestly diminished the amplitude of the Ca^{2+} wave (see the blue lines Fig. 1D). These data confirmed that sperm-induced CF in *P. lividus* eggs involves Ca^{2+} influx through voltage-gated L-type Ca^{2+} channels, as has been suggested in other species of sea urchin and starfish.

3.2. Depleting the GPN-sensitive Ca^{2+} store in sea urchin eggs leads to substantial inhibition of the cortical flash, abnormal FE elevation, and polyspermy.

When sea urchin eggs microinjected with the caged NAADP are exposed to UV, an abrupt Ca^{2+} increase confined to the cortex propagates as a Ca^{2+} wave towards the inner cytoplasm [6]. This cortical Ca^{2+} increase, which closely resembled the CF during fertilization, was later suggested to originate from the acidic vesicles (i.e. YG) [5]. To test whether this intracellular Ca^{2+} store contributes to the CF, we applied GPN to specifically deplete it before fertilization. Pretreatment of sea urchin (*P. lividus*) and starfish (*Astropecten aranciatus*) eggs to osmotically rupture the membrane of acidic vesicles, produced random but localized Ca^{2+} bursts in the egg periphery, suggesting that the GPN-susceptible vesicles contain Ca^{2+} (Supplemental data 1) as was shown in the other species of sea urchin [5]. When fertilized, sea urchin eggs preincubated with GPN (200 μM , 40 min) displayed changes in the peak

amplitude of the Ca²⁺ wave (0.31 ± 0.07 RFU, n=14) in reference to the control eggs from the same batch pretreated with 0.05 % DMSO (0.38 ± 0.07 RFU, n=12; P<0.05) (Fig 2B). In addition, GPN pretreatment significantly diminished the planar velocity of the Ca²⁺ wave (3.84 ± 0.38 μm/sec, n=14) as compared to

control eggs (4.76 ± 0.65 μm/sec, n=12; P<0.001), and accelerated the decline of the Ca²⁺ levels to the baseline values (0.072 ± 0.034 RFU) as opposed to average values in the control eggs (0.254 ± 0.051 RFU; P<0.001) measured 3 minutes after the initial Ca²⁺ signal was detected (Fig. 2B).

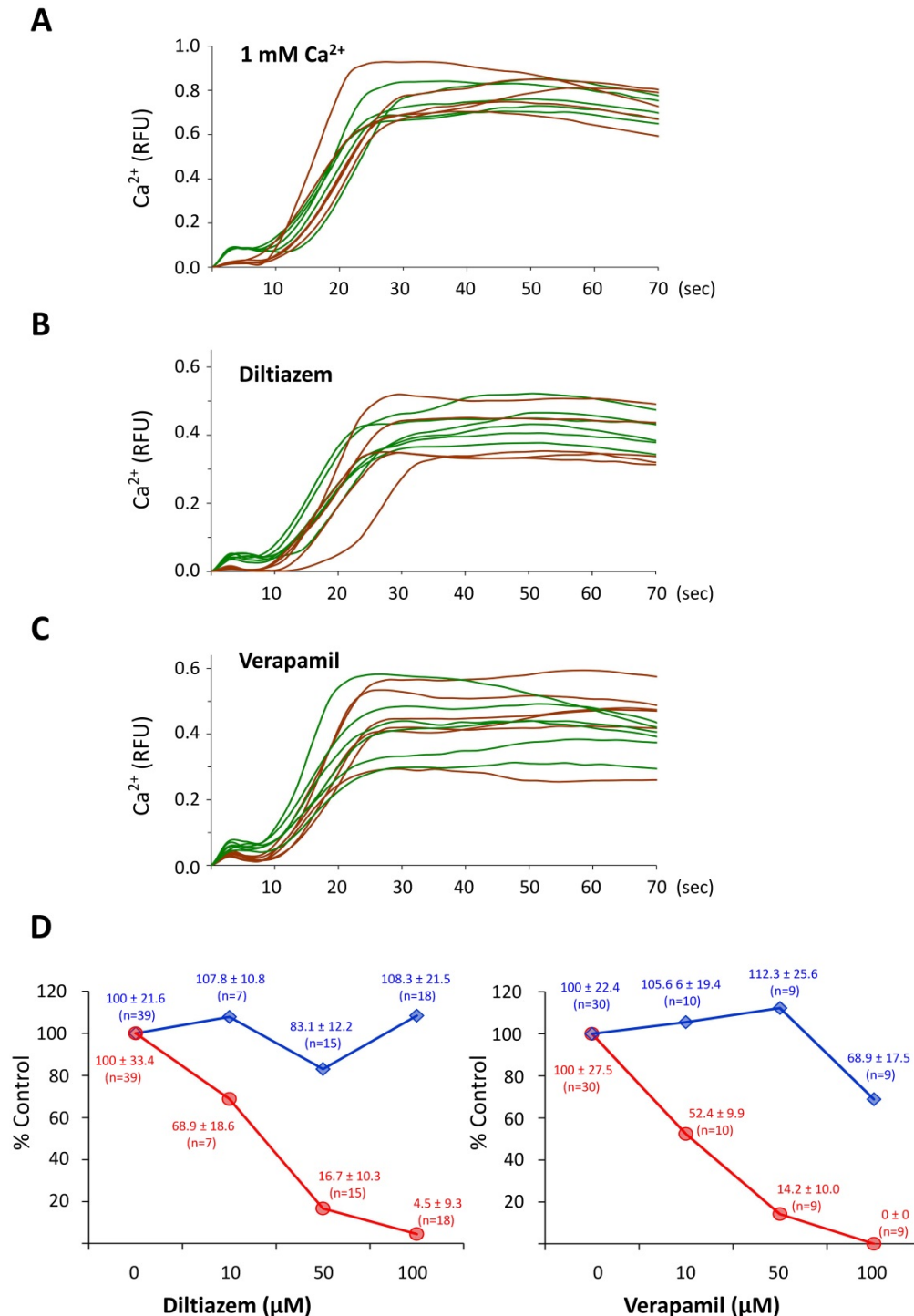


Figure 1. The cortical flash depends on the Ca²⁺ influx via L-type Ca²⁺ channels. (A) The eggs fertilized in the ASW with 1 mM Ca²⁺ (brown curves) displayed virtually the same Ca²⁺ response as in control eggs (ASW with 10 mM Ca²⁺, green curves), but the CFs were severely suppressed. (B-C) *P. lividus* eggs were pretreated with either diltiazem or verapamil for 40 minutes, and their Ca²⁺ responses at fertilization were compared with that of control eggs (FSW) in the same batch. The trajectories of the Ca²⁺ levels in the fertilized eggs that had been pretreated with 50 μM diltiazem or 10 μM verapamil were shown in brown curves, whereas the responses in the control eggs were presented in green curves. (D) The dose-dependent effects of diltiazem and verapamil on the Ca²⁺ signalling in fertilized eggs. The peak amplitudes of the CF (red line) and the global Ca²⁺ increase (blue line) in the eggs pretreated with varied amount of diltiazem and verapamil were normalized with the corresponding average levels in the control eggs of the same batch.

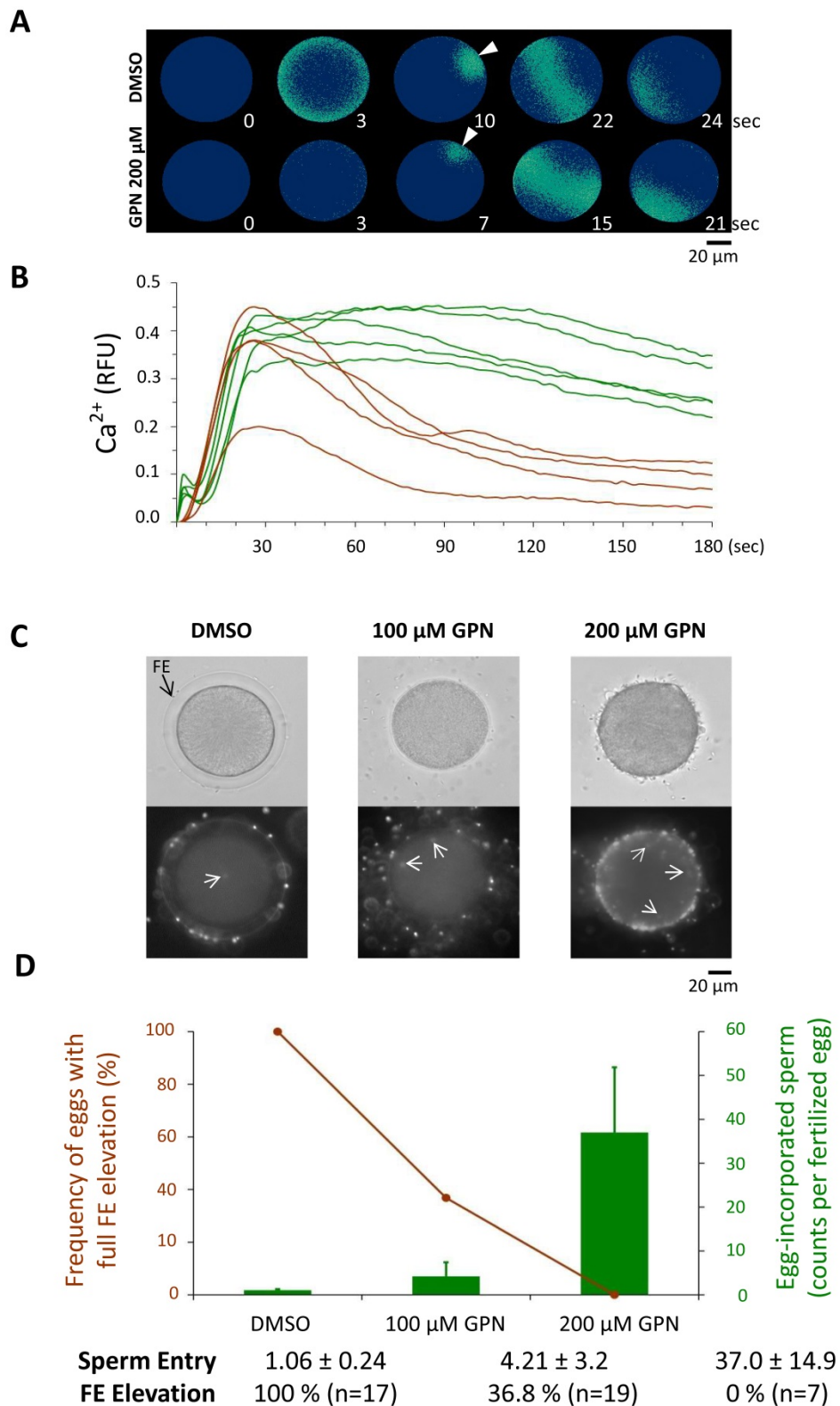


Figure 2. Fertilization of the sea urchin eggs pretreated with GPN. *P. lividus* eggs were fertilized following the pretreatments described in the Materials and Methods. (A) Pseudocolor images of the instantaneous changes of the Ca²⁺ signals at several key moments of the propagating wave in representative eggs. The arrow indicates the intracellular Ca²⁺ increase at the spot of the sperm-egg interaction site. (B) The quantified Ca²⁺ increases in the control (green curves) and GPN-pretreated (200 μM, brown curves) eggs in one of the four independent experiments. (C) Dose-dependent effects of GPN on the elevation of the FE and polyspermy. Sperm inside the fertilized eggs were visualized with the Hoechst 33342 (arrows), scale bar 20 μm. (D) The average numbers of the egg-incorporated spermatozoa were provided as Mean ± SD (bars) and the FE elevation as a frequency (line).

These observations might suggest that the Ca²⁺ ions stored in the GPN-susceptible vesicles somehow

contribute to the Ca²⁺ wave at fertilization. However, the strongest effect of GPN was observed on the

amplitude of the CF. In the same GPN-pretreated eggs, the CFs were barely detectable at fertilization, as their average amplitude was reduced to merely 0.004 ± 0.005 RFU, whereas the average CF detected in the batch-matching control eggs was 0.064 ± 0.024 RFU, $P < 0.001$. Furthermore, with the loss of GPN-susceptible cortical vesicles that would otherwise participate in exocytosis, these eggs often failed to fully elevate the FE, and incorporated supernumerary spermatozoa in a dose-dependent manner (Fig. 2C and D). Whereas the frequency of the eggs displaying fully elevated FE was 100 % in the control eggs pretreated with 0.05 % DMSO ($n=17$), the rates in the eggs pretreated with 100 and 200 μM GPN were reduced to 36.8 % ($n=19$) and 0 % ($n=7$) (Fig. 2C), respectively. In the same experiment, the control eggs were mostly monospermic, as the average number of the egg-incorporated sperm at fertilization was 1.06 ± 0.24 ($n=17$). By contrast, in the eggs pretreated with 100 and 200 μM GPN, the internalized sperm counts were greatly increased to 4.21 ± 3.20 ($n=19$; $P < 0.001$ compared with the control) and 37.0 ± 14.9 ($n=7$; $P < 0.01$ compared with the eggs pretreated with 100 μM GPN), respectively (Fig. 2C and D). Thus, depletion of the GPN-susceptible Ca^{2+} store caused inhibition of the CF, a reduction of the peak amplitude of the Ca^{2+} wave, as well as an increased rate of polyspermy and failure of the FE elevation.

3.3. GPN disrupts the acidic vesicles stained with LysoTracker-RED and causes fusion of the CG with the adjacent vesicles.

In *Lytechinus pictus* eggs, it was reported that GPN eliminates the acidic vesicles stained with LysoTracker-RED [5]. To test if GPN actually disrupts a population of acidic vesicles in *P. lividus* eggs as well, sea urchin eggs exposed to 10 nM LysoTracker-RED for 1 h were incubated in the presence of 200 μM GPN. After 40 minutes, some of

these eggs were fertilized to follow the fate of the LysoTracker-RED-positive vesicles. As shown in Fig. 3A, GPN eliminated the fluorescent signals coming from the LysoTracker-RED-stained vesicles (see the red dots) in comparison with the control eggs exposed to DMSO, which retained red dots all over the cytoplasm. Curiously, the number of acidified vesicles visualized by LysoTracker-RED was increased throughout the cytoplasm following fertilization. This tendency was evident in both control and GPN-treated eggs by 25 minutes after fertilization, which might represent the changes linked to the uptake of H^+ into the vesicles during the course of alkalization of the cytosol after fertilization [22]. We then examined the effect of GPN on the ultrastructure of the egg cortex before and after fertilization. In line with the loss of a population of acidic vesicles visualized by LysoTracker-RED, the egg cortex viewed by transmission electron microscopy (TEM) displayed corresponding changes. First, GPN dislodged CG from the vicinity of the plasma membrane in unfertilized eggs. The membrane-bound CG in the control eggs (red arrow) apparently underwent exocytosis and were not visible anymore after fertilization (Fig. 3B). In the eggs pretreated with GPN, some CG were either positioned deeper in the cytoplasm or displayed signs of fusion among themselves (white arrows) or with other vesicles (black arrow) (Fig. 3B). The EM image of the fertilized eggs after GPN pretreatment showed that the FE was elevated only partially, and that the microvilli extension in the perivitelline space was barely detectable (Fig. 3B). Hence, these data suggest that GPN-induced changes in CF and the Ca^{2+} wave in the fertilized eggs of sea urchin (Fig. 2) might be linked to the alteration of the CG and microvilli structures in the cortex.

Table 1. Microvilli count on the surface of the *P. lividus* eggs.

Treatment	Microvilli shape		Average microvilli count per treatment *	Comparison with control eggs	
	Normal (%)	Abnormal (%)		Shape change	counts
FSW (control)	99.06	0.94	179.9 (n=4)	n/a	n/a
Urethane 400 mM	88.96	11.04	118.7 (n=4)	$P < 0.001$	$P < 0.001$
Procaine 10 mM	82.39	17.61	112.3 (n=4)	$P < 0.001$	$P < 0.001$
NH ₄ Cl 40 mM	88.61	11.39	132.5 (n=4)	$P < 0.001$	$P < 0.01$
Stratified	83.16	16.84	84.6 (n=4)	$P < 0.001$	$P < 0.001$
DMSO (control)	98.51	1.49	230.1 (n=4)	n/a	n/a
GPN 200 μM	85.88	14.12	112.1 (n=4)	$P < 0.001$	$P < 0.001$
FSW (control)	99.64	0.36	324.83 (n=2)	n/a	n/a
Diltiazem 50 μM	94.1	5.82	265.91 (n=4)	$P < 0.01$	$P < 0.05$
Verapamil 50 μM	91.95	8.05	273.5 (n=4)	$P < 0.01$	$P < 0.05$

* Microvilli counted from three separate regions (26.1 μm^2) randomly selected from 2 to 4 different eggs for each experiment. n/a, nonapplicable.

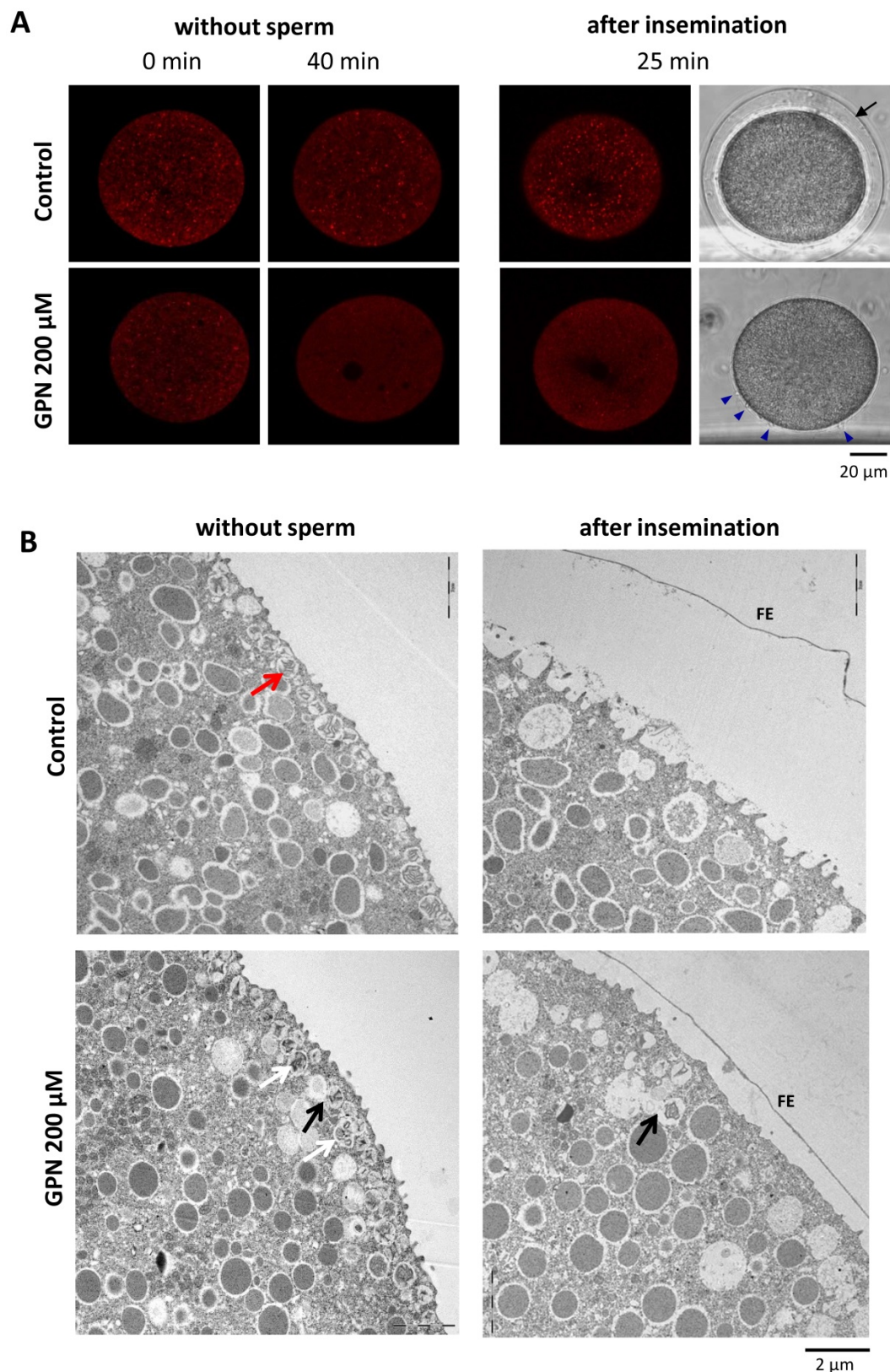


Figure 3. Effect of GPN pretreatment on the CG and vesicles. (A) *P. lividus* eggs were stained with LysoTracker-RED before and after (40 min) the treatment with 200 μ M GPN or DMSO (control), and viewed in confocal microscopy. The changes of the fluorescent signals in the LysoTracker-RED-stained vesicles were examined in the same eggs 25 minutes after fertilization. Control eggs displayed full elevation of the FE, but most eggs treated with GPN failed at the FE elevation despite the formation of multiple fertilization cones (blue arrowheads). **(B)** Electron micrographs of the cortex of the eggs treated with 200 μ M GPN or DMSO. In control eggs, cortical granules (red arrow) positioned underneath the plasma membrane were all exocytosed into the perivitelline space 5 minutes after fertilization (right panel). In GPN-pretreated eggs, CG appeared to fuse with each other (white arrow) or with the adjacent vesicles (black arrow), and to be displaced from the plasma membrane. After insemination, FE elevates only partially while some CG fused with other granules (black arrow) are still visible inside the eggs.

3.4. GPN, verapamil and diltiazem cause drastic reorganization of microvilli on the egg's surface.

As the partial FE elevation in the GPN-pretreated eggs (Fig. 3B) can be due to the incomplete CG exocytosis or to the failed extension of microvilli [13], we examined microvillar morphology on the egg surface by scanning electron microscopy (SEM). We found that the microvilli covering the surface of the *P. lividus* eggs pretreated with 200 μ M GPN were nearly twofold lower in number and bore irregular shapes that may signify bending, overextension, or fusion. In contrast, the DMSO-treated control eggs manifested microvilli with rather uniform length and distribution (Fig. 4A, Table 1). After fertilization, the control eggs pretreated with DMSO showed elevation of an intact FE on the surface, to which a spermatozoon is seen to be attached (Supplementary data S2). On the other hand, the eggs fertilized after GPN pretreatment manifested multiple cracks on the surface of FE (Supplementary data S2, arrow). Hence, GPN not only changes the vesicles and granules in the egg cortex, but also alters the egg surface and functionality of the microvilli. As the treatment with GPN caused significant changes in the shape and number of microvilli together with specific inhibition of the CF, we tested if the conventional inhibitors of L-type voltage-gated Ca^{2+} channels would have the same effect on microvilli. Interestingly, we found that diltiazem and verapamil both increased the percentage of microvilli with the irregular shapes as in the GPN-pretreated eggs, and that the numbers of microvilli in the unit area were significantly reduced in comparison with the control eggs from the same batch (Fig. 4B, Table 1). Hence, the structural changes in microvilli may add to the pharmacological effects of these two inhibitors of L-type Ca^{2+} channels at least in the sea urchin eggs. Not having affected cortical vesicles, eggs pretreated with verapamil and diltiazem underwent normal CG exocytosis at fertilization and exhibited full elevation of the FE (data not shown).

3.5. SEM and TEM observations of *P. lividus* eggs treated with agents dislocating CG.

As an experimental paradigm slightly different from GPN which ruptures CG, we dislodged CG and clear vesicles from the plasma membrane to see if such changes would have the same effects on the Ca^{2+} signaling. To this end, *P. lividus* eggs were exposed to procaine, urethane and ammonia and the morphological modifications of the egg surface were examined by electron microscopy. The TEM image of the untreated eggs normally displayed orderly

monolayer of CG underneath the plasma membrane (Fig. 5A, red arrow). By contrast, as with *Arbacia punctulata* eggs, *P. lividus* eggs treated with urethane (400 mM) or procaine (10 mM) showed numerous CG somewhat smaller and displaced away from the plasma membrane, often forming multiple layers (e.g. compare the size and arrangement of the CG marked with red arrows in Fig. 5). In addition, unlike the control eggs, the surface of the eggs pretreated with urethane or procaine was highly corrugated or undulated with numerous invaginations and protrusions (Fig. 5B and C, black arrow). Similarly, dislocation of the CG from the outer region of the egg cortex (red arrows) was also observed in the eggs pretreated with NH_4Cl (pH 9.0), but this treatment did not much change the egg's contour nor the size of CG. Nonetheless, it has been demonstrated that urethane, procaine, and NH_4Cl induce structural changes in the microvilli and subplasmalemmal layer of sea urchin eggs (*Strongylocentrotus purpuratus* and *Arbacia punctulata*), as judged by fluorescent probes for F-actin [45]. In line with that, our SEM data revealed significant changes in the structure of microvilli in the eggs treated with the same agents (Fig. 5, SEM). After being exposed to 400 mM urethane for 5 minutes, the microvilli on the corrugated surface of *P. lividus* eggs took irregular shapes (Fig. 5B, SEM). On the other hand, eggs exposed to 10 mM procaine for 30 minutes showed considerable reduction in the microvilli number with increased frequency of the irregularly shaped microvilli (Fig. 5C, Table 1). Finally, the microvilli of the eggs treated with 40 mM NH_4Cl (pH 9.0) for 30 minutes displayed morphological alteration with slightly elongated or twisted shape, but again with reduced density per unit area (Fig. 5D, Table 1). Thus, besides CG dislocation, which represented the common feature of the three pretreatments, microvilli were reduced in number while the frequency of the irregularly-shaped microvilli was increased (Table 1). Hence, in these conditions, the fertilizing sperm is met by a strikingly different egg with completely reorganized cell surface.

3.6. Effects of urethane, procaine, and NH_4Cl on the sperm-induced Ca^{2+} signals.

Once dislodged and relocated, the CG lose their contact with the plasma membrane in an altered cytoskeletal environment, as was seen in the microvilli. Thus, we examined the physiological consequence of such structural changes. When fertilized, the eggs pretreated with urethane, procaine and NH_4Cl exhibited consistent changes in certain aspect of intracellular Ca^{2+} signaling (Table 2 and Fig. 6). In short, neither of the treatment affected the

amplitude of the global Ca^{2+} increase, indicating that CG dislocation and the alteration of microvilli do not substantially perturb the generation of the Ca^{2+} wave, whereas rupturing CG with GPN did so. Nonetheless, the eggs pretreated with procaine or NH_4Cl exhibited much faster declining kinetics of the intracellular Ca^{2+} level after fertilization (Fig. 6). In addition, eggs pretreated with urethane and procaine displayed slightly faster and slower planar velocity of the Ca^{2+} wave, respectively (Table 2). These observations might have several implications about the possible

rearrangement of the components constituting the 'excitable cytoplasmic media' that either transmit or buffer the Ca^{2+} wave after CG dislocation (see Discussion). More importantly, in all these eggs with CG relocation and microvilli changes, the amplitude of the sperm-induced CF was significantly suppressed. Extending the data with GPN, these results suggest that close association of CG with the plasma membrane and the normal shape and distribution of microvilli may be important for the generation of the CF and the Ca^{2+} wave.

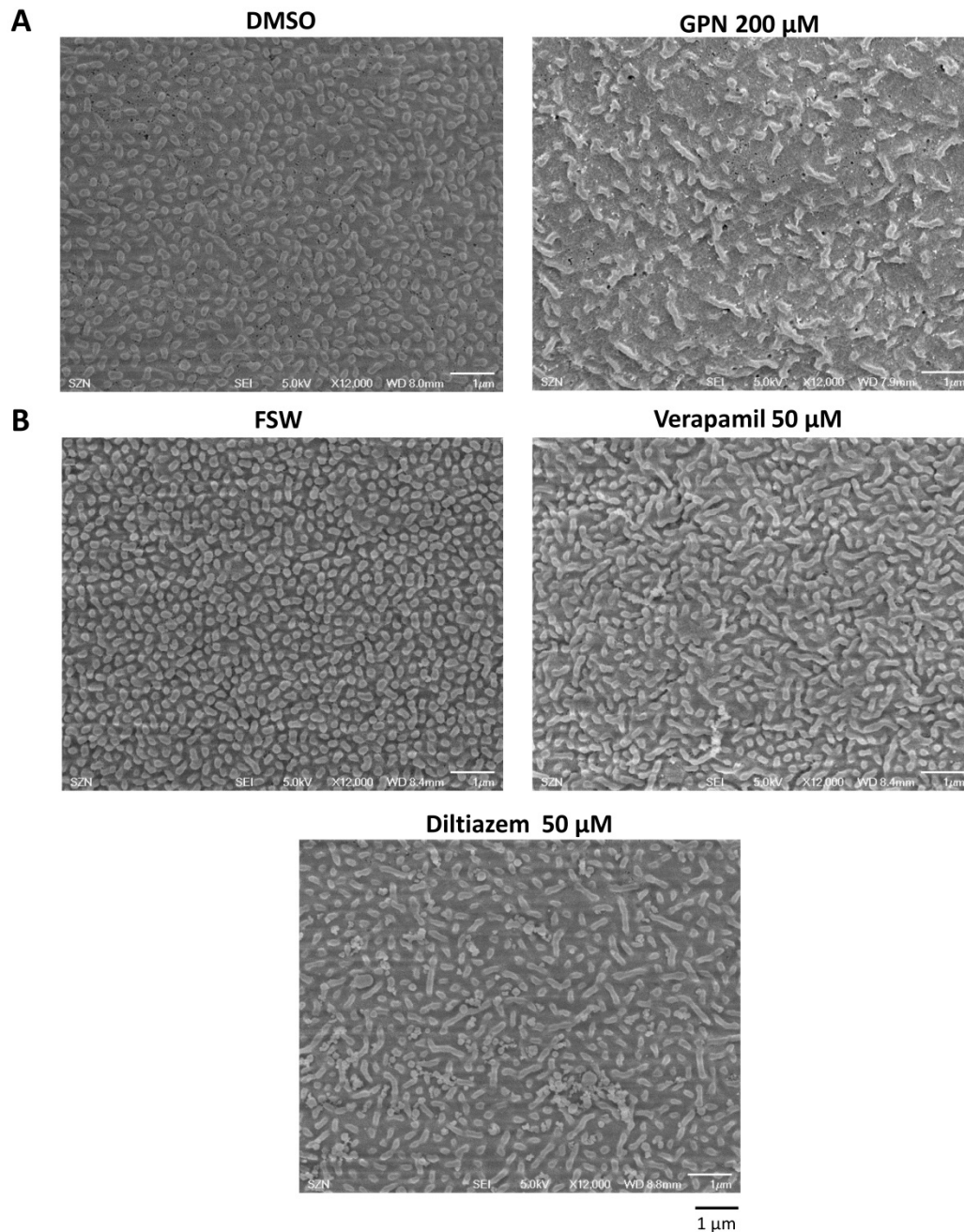


Figure 4. Ultrastructural changes of the egg surface after the treatment with GPN, diltiazem and verapamil. (A) SEM images showing the microvilli of the unfertilized eggs treated with GPN (200 μM , 40 min) and DMSO. Note the reduced density of microvilli and their elongated shape in GPN-treated eggs in comparison with the control egg exhibiting regularly dispersed and shorter microvilli. **(B)** Effects of verapamil (50 μM , 40 min) and diltiazem (50 μM , 40 min) on the microvilli structure and quantity. Whereas SEM images of the control egg (FSW) display microvilli of regular distribution and length, the microvilli of the eggs treated with the two L-type Ca^{2+} channel inhibitors show irregular shapes and reduced quantity (also see Table 1). Scale bar 1 μm .

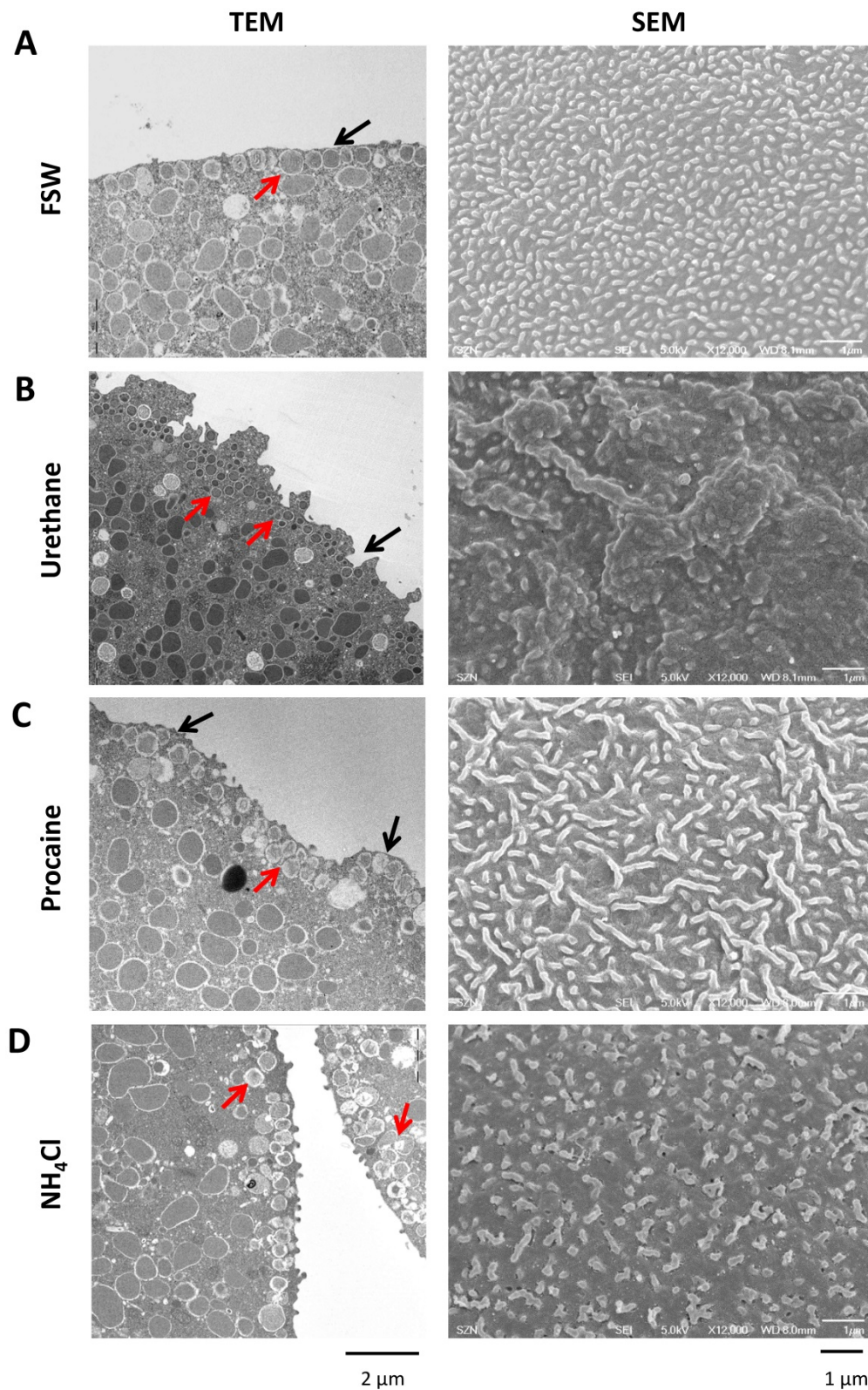


Figure 5. Effects of urethane, procaine and NH₄Cl on the ultrastructure of the egg surface. (A) TEM and SEM images of *P. lividus* control eggs show dense microvilli with nearly uniform shape and size. In the TEM image (left panel), CG are apparently attached to the plasma membrane. (B) After urethane treatment (400 mM, 5 min), egg surface shows a sign of corrugation and significant loss of microvilli (SEM). The treatment induces invaginations on the egg surface and dislocation of some CG from the plasma membrane (TEM, black arrow). (C) Incubation with procaine (10 mM, 20 min) gives rise to microvilli elongation as well as reduction in their number. Some parts of the cell surface are deprived of microvilli (SEM, right panel). Procaine-pretreated eggs show bulges on the surface (black arrow) and some CG lost their attachment to the plasma membrane (red arrow) to form a secondary layer. (D) NH₄Cl-treatment (40 mM pH 9.0, 30 min) shows loss of microvilli and changes in their shape (SEM) as well as translocation of some CG (TEM, red arrows).

Table 2. Intracellular Ca²⁺ increase in fertilized sea urchin eggs pretreated with urethane, procaine and NH₄Cl.

	Fertilization				Ca ²⁺ decline level (RFU)		VL Elevation %			n
	Cortical flash	Latent period (sec)	Global Ca ²⁺ (RFU)	Planar velocity (μm/sec)	3 min post-fertilization	Full	Partial	None		
Control (FSW)	0.068 ± 0.023	8.4955 ± 4.755	0.445 ± 0.097	5.0204 ± 0.6601	0.2808 ± 0.0623	60.8	30.5	8.7	23	
Urethane 400 mM	0.051 ± 0.017	7.0422 ± 5.2904	0.4204 ± 0.075	5.8657 ± 1.2344	0.2141 ± 0.0739	86.3	9.1	4.6	22	
T-test	< 0.05	0.3374	0.341	< 0.01	< 0.01					
Control (FSW)	0.087 ± 0.013	10.33 ± 4.736	0.412 ± 0.066	5.0447 ± 2.0975	0.2769 ± 0.0675	72.7	27.3	0	11	
Procaine 10 mM	0.0347 ± 0.017	11.125 ± 5.15	0.472 ± 0.081	3.2696 ± 0.3560	0.1231 ± 0.1033	0	0	100	9	
T-test	< 0.001	0.7236	< 0.05	< 0.05	P < 0.001					
Control (FSW)	0.066 ± 0.016	8.934 ± 2.396	0.361 ± 0.049	3.4338 ± 0.5819	0.227 ± 0.042	72.7	18.2	9.1	11	
NH ₄ Cl 40 mM	0.042 ± 0.028	8.415 ± 4.095	0.348 ± 0.088	3.4263 ± 0.9704	0.0816 ± 0.0257	0	44.4	55.6	9	
T-test	< 0.05	0.7279	0.6764	0.9832	< 0.001					

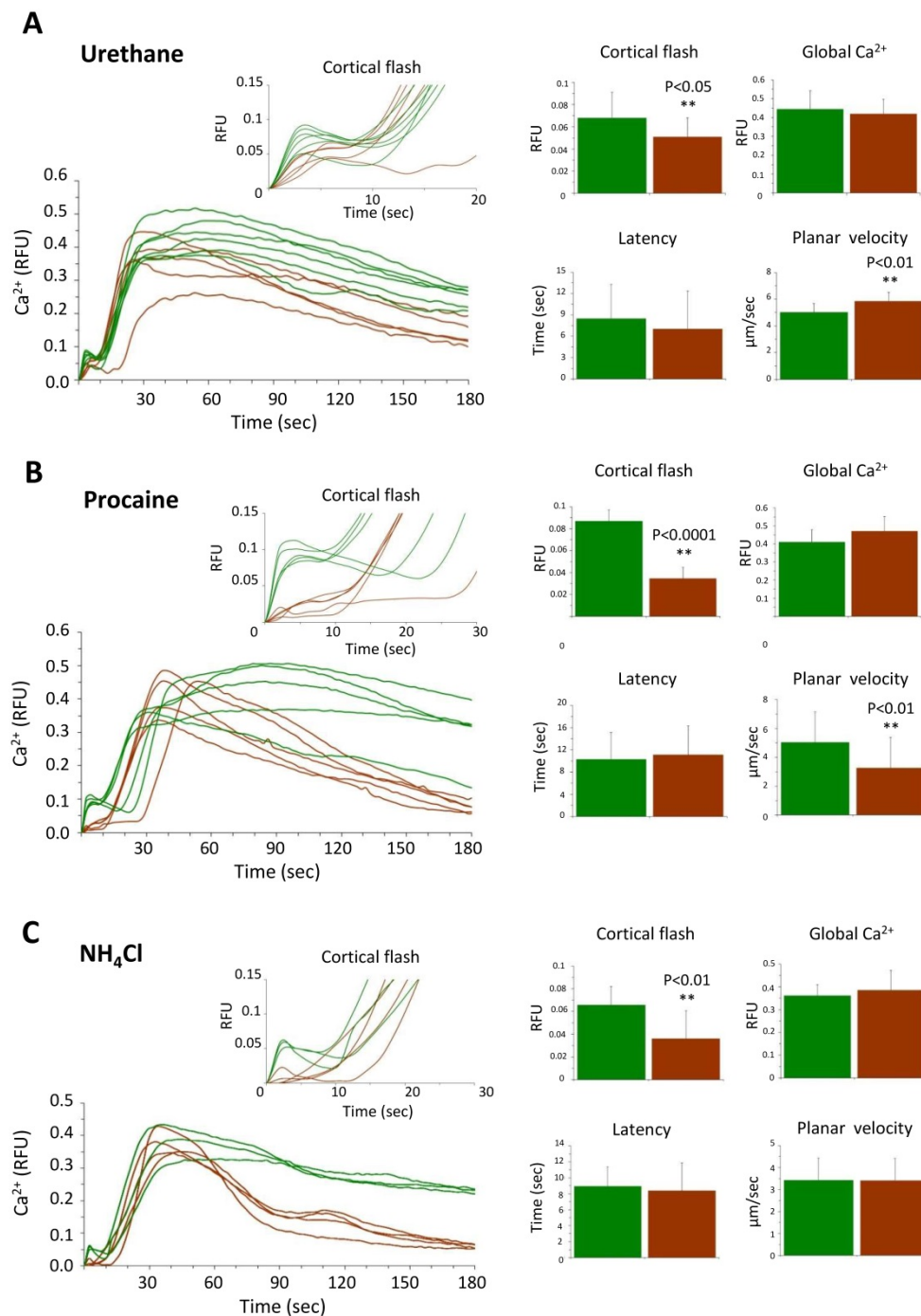


Figure 6. Effects of urethane, procaine and NH₄Cl pretreatment on the Ca²⁺ signaling at fertilization. (A) Ca²⁺ response in the *P. lividus* eggs pretreated with 400 mM urethane for 5 minutes, (B) 10 mM procaine for 20 minutes and (C) 40 mM NH₄Cl (pH 9.0) for 30 minutes prior to fertilization. The Ca²⁺ trajectories after fertilization of the same batch of control and treated eggs are presented, and various parameters of the intracellular Ca²⁺ increase are shown with histograms as average values from three independent experiments. The experimental data are summarized in Table 2.

3.7. Sperm-induced Ca²⁺ signals in the stratified eggs of *P. lividus*.

Now that CG are important for the generation of CF at fertilization, we asked whether other Ca²⁺-storing acidic vesicles (e.g. YG) could contribute to the sperm-initiated Ca²⁺ increase in sea urchin eggs. To that end we stratified *P. lividus* eggs by centrifugation in a physical condition that dislodge and redistribute the egg organelles to certain

subcellular regions [30]. While CG still remain bound to the plasma membrane in this condition, clear vesicles, the nucleus and the ER translocate towards the centripetal pole, whereas the YG and the mitochondria to the centrifugal egg pole [22]. Firstly, we noted that the surface of the elongated eggs after centrifugation was corrugated (Fig. 7B) and the density of microvilli significantly decreased (Table 1).

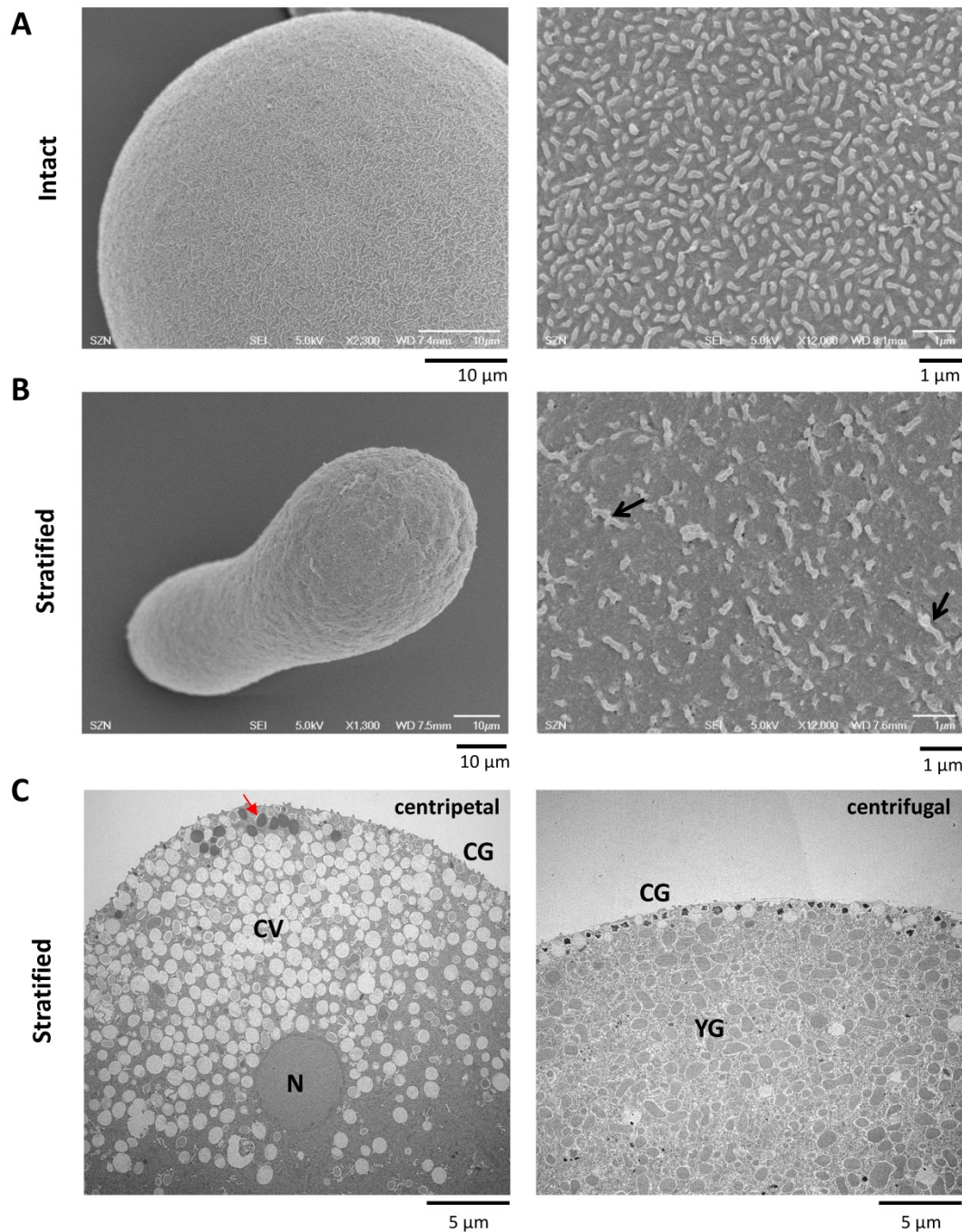


Figure 7. Effects of sea urchin egg stratification on microvilli structure and egg surface. (A) Intact sea urchin eggs viewed by SEM in low (left panel) and high magnification (right). Note the microvilli covering the surface. (B) Centrifugation stretches the eggs (left panel), corrugates the surface and diminishes the density of microvilli (right panel) (see Table 1). Some of the thickened and elongated microvilli are indicated with arrows. (C) TEM image of a centrifuged egg at the centripetal (left) and centrifugal side (right). While CG are still aligned underneath the plasma membrane in both sides, the cytoplasm at the centripetal and centrifugal sides are predominantly occupied with clear vesicles (CV) and yolk granules (YG), respectively. A minor class of less characterized vesicles enriched with highly electron-dense contents are marked with red arrow. N, nucleus.

Furthermore, the microvilli in the stratified eggs appeared thicker and longer with irregular shapes (Fig. 7B, Table 1), whereas the CG attained their apparent attachment to the plasma membrane as observed with the TEM (Fig. 7C). When the stratified eggs were fertilized, the Ca^{2+} increase at the time of CF was most prominent in the narrow centrifugal pole where YG are localized and ER is scarce (Fig. 7C and 8A). As a whole, however, the average amplitude of the CF manifested by the stratified eggs was

marginally reduced with high variability (0.09 ± 0.04 RFU, $n=11$) in comparison with the control (0.14 ± 0.01 RFU, $n=13$; $P=0.0598$) (Fig. 8B). This modest decrease in the amplitude of CF despite the considerably large Ca^{2+} increase localized in the centrifugal pole (Fig. 8A) suggests that there might be a general tendency of suppressing CF in the rest of the cell surface, as implied by the significantly reduced microvilli density on the surface (Table 1).

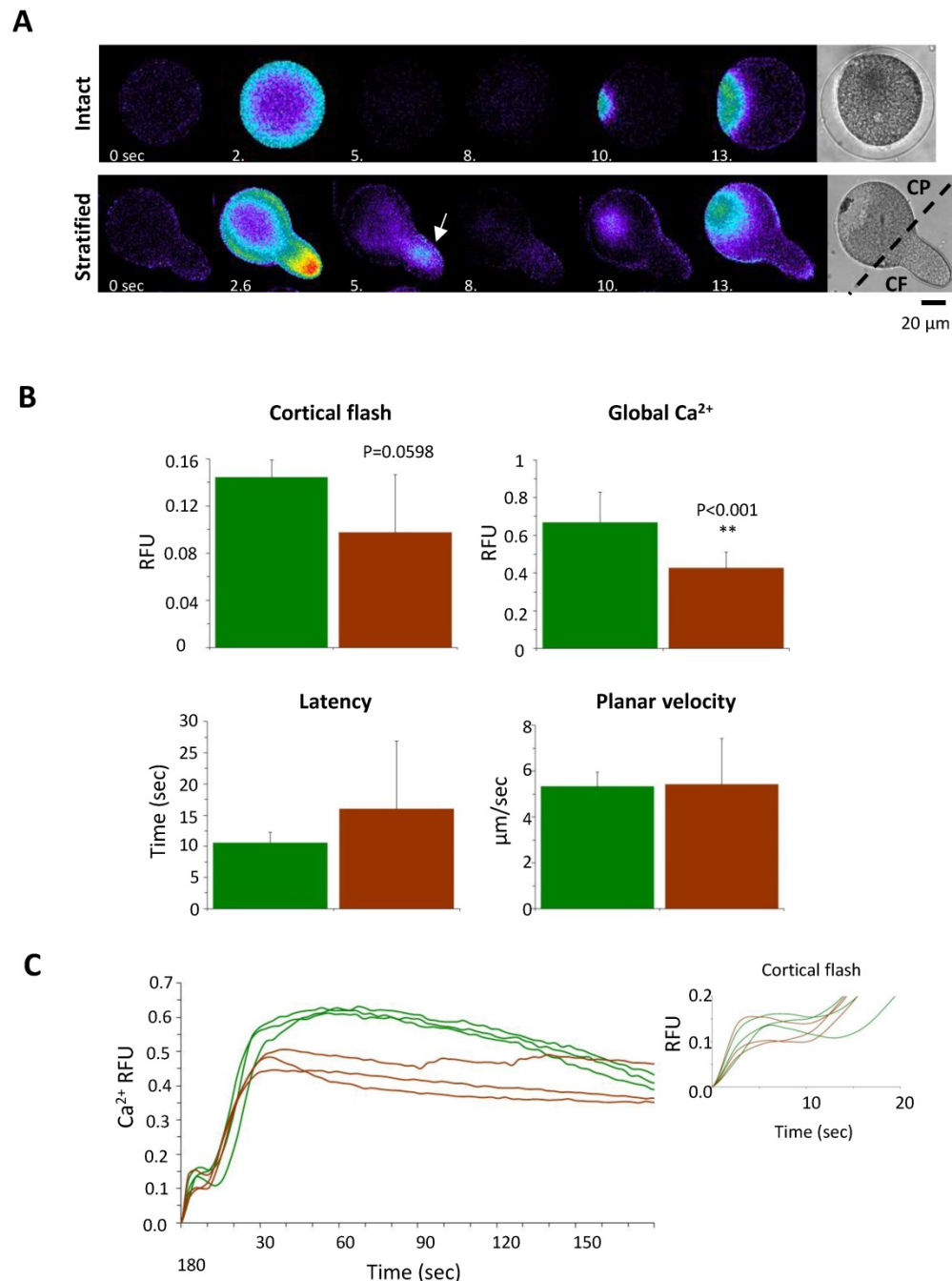


Figure 8. The Ca^{2+} response in the stratified eggs at fertilization. (A) Pseudo-colored images showing the CF and the beginning of the sperm-initiated Ca^{2+} wave in intact and centrifuged eggs of *P. lividus*. Note the secondary calcium increase during the CF (at 5.3 sec) in the centrifugal pole of the centrifuged egg (arrow). Scale bar 20 μm . **(B)** Comparison of various aspects of the Ca^{2+} signaling in the intact and stratified eggs. See the text in Results for detail. **(C)** Calcium curves at fertilization in intact (green) and stratified eggs (brown) from one batch of experiments demonstrating the suppression of the Ca^{2+} wave in stratified eggs (brown).

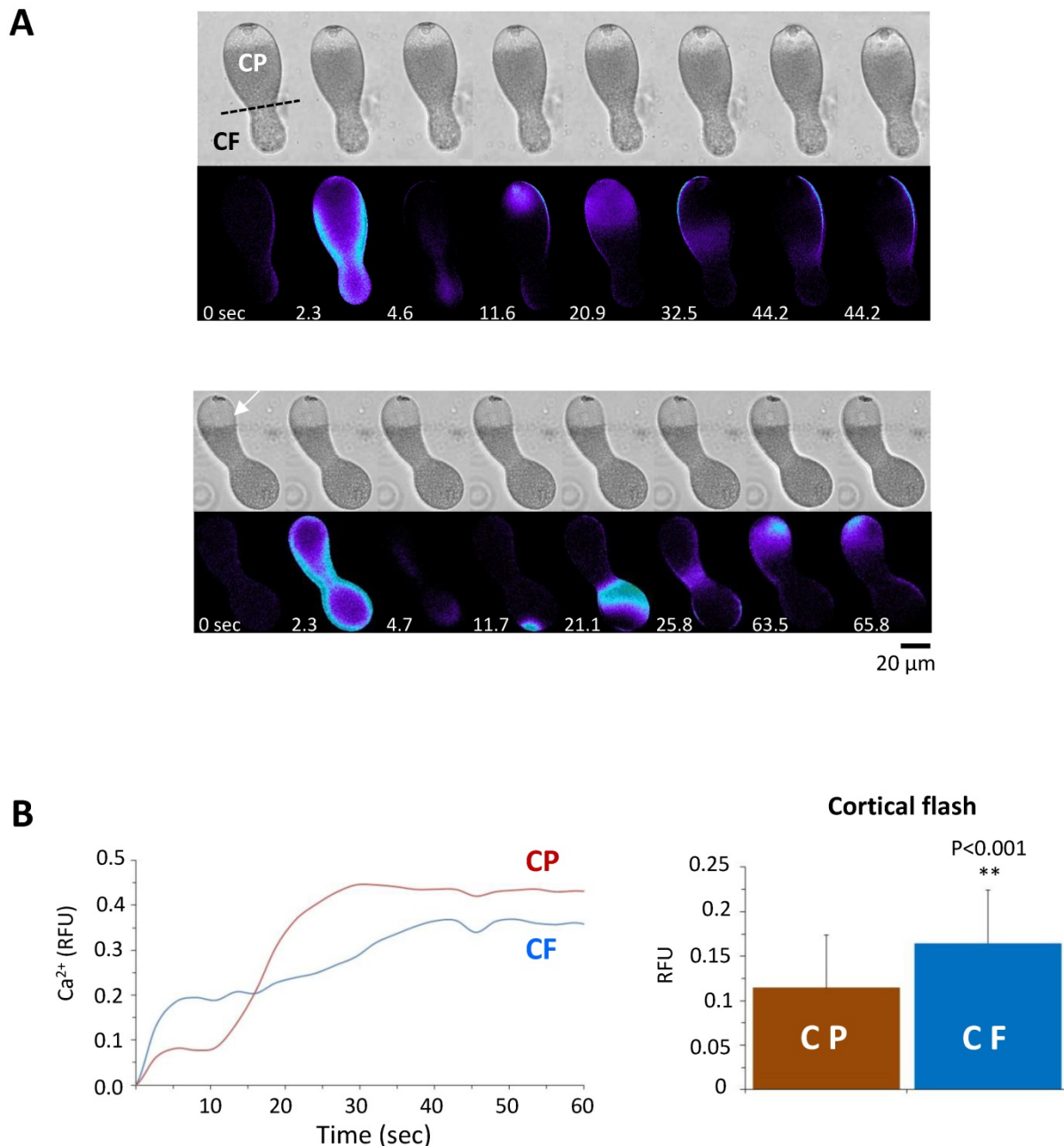


Figure 9. Comparison of the Ca^{2+} responses at fertilization in the centrifugal and centripetal halves of the stratified eggs. (A) Pseudocolor images of stratified eggs at fertilization showing the sperm's ability to induce Ca^{2+} increase from both centripetal (CP) and centrifugal (CF) sides of the eggs. **(B)** Representative Ca^{2+} curves of the sperm-initiated CFs in the centrifugal (blue line) and centripetal (red line) poles of stratified eggs. The histograms represent the average amplitude of the CF in stratified eggs, which was significantly higher in the centrifugal (0.16 ± 0.06 RFU, $n=27$) compared to the centripetal pole (0.11 ± 0.05 RFU, $n=27$; $P<0.001$).

On the other hand, the peak amplitude of the Ca^{2+} wave in the stratified eggs (0.43 ± 0.08 RFU, $n=11$) was significantly lower than the values in the intact eggs from the same batch (0.67 ± 0.16 RFU, $n=13$; $P<0.001$), but the accelerated decline of the intracellular Ca^{2+} level was not observed unlike the eggs pretreated with agents dislocating or disrupting CG (Fig. 8B and C). Interestingly, the polarized redistribution of the Ca^{2+} stores such as ER in the stratified eggs did not lead to clear preference with respect to the origin of sperm-induced Ca^{2+} wave.

When fertilized, 53.9 % of the stratified eggs ($n=21$) triggered the sperm-induced Ca^{2+} wave from the centripetal pole where the nucleus and ER are located (Fig. 9A). Surprisingly, nearly half (46.1%) of the stratified eggs ($n=18$) initiated the Ca^{2+} wave from the centrifugal side where ER is relatively scarce (Fig. 9A and B). As ER is assumed as the primary internal store affording the Ca^{2+} wave in fertilized eggs, this result suggests that at least the initial Ca^{2+} being liberated during the wave generation might not necessarily derive from ER. Nonetheless, the stratified eggs with

polarized distribution of the internal Ca^{2+} stores exhibited differential Ca^{2+} rise at fertilization. When the CF was further assessed in the two parts of the stratified eggs regardless of the site of sperm fusion, the amplitude of the CF was again always significantly higher in the centrifugal half where YG are preferentially located (Fig. 9B). Importantly, we noted that the way CF is generated in the two halves were apparently distinct from each other. While the CF in the centripetal half appears to proceed in one phase, the initial burst of the Ca^{2+} beneath the plasma membrane in the centrifugal half is immediately followed by a secondary Ca^{2+} increase in the subjacent cortex (Fig. 8A; Fig. 9A and B). This in part explains why the amplitude of the CF in centrifugal half (0.16 ± 0.06 RFU, $n=27$), where YG are located, was significantly higher than that in the centripetal half (0.11 ± 0.05 RFU, $n=27$; $P<0.001$) (Fig. 9B). This observation raises the possibility that, in theory, YG can enhance the Ca^{2+} increase during the later stage of CF at fertilization.

4. Discussion

The cortex of sea urchin egg is crowded with various granules and vesicles that are known to contain Ca^{2+} in their lumen. In this manuscript, we have examined their potential contribution to the intracellular Ca^{2+} signaling during the initial phase of fertilization. While CF mainly represents Ca^{2+} influx from outside through L-type Ca^{2+} channels (Fig. 1), the data presented in this communication suggest that the sperm-induced Ca^{2+} signals are somehow affected by cortical structural modifications such as ablation or dislocation of CG and other vesicles in the subplasmalemmal region, as well as by the changes in the number and morphology of the microvilli. Firstly, the fusion and disruption of vesicles in the egg cortex by GPN led to severe reduction in the amplitude of the CF and a faster Ca^{2+} wave decline (Fig. 2B). This treatment led to no or partial elevation of the FE, indicating that GPN may rupture not only YG, as previously reported [5,29], but also the CG. Unlike GPN, treatment of *P. lividus* eggs with urethane, procaine, and NH_4Cl simply dislodged CG away from the plasma membrane (Fig. 5). Also in these eggs, the amplitude of the CF was severely reduced, while the peak of the Ca^{2+} wave was not much affected (Fig. 6). Nonetheless, as with the GPN-pretreated eggs, the decay phase of the Ca^{2+} wave in these eggs (especially the ones pretreated with procaine and NH_4Cl) was notably faster in dropping to the basal level (see the brown curves in Fig. 6 after the Ca^{2+} peak, Table 2). This consistent observation might be attributed to the spatial and structural modifications of the vesicles and granules which might have rendered these

vesicles and granules more efficient as Ca^{2+} -re-uptaking stores. Alternatively, the same result might reflect failure of a secondary Ca^{2+} -releasing mechanism whose potential action during the late phase of Ca^{2+} increase is masked by the massive Ca^{2+} increases caused by InsP_3 or cADPr . A potential candidate player in the latter scenario is the ion channels involved in store-operated Ca^{2+} entry (SOCE) [46]. Although such a mechanism has been controversial in sea urchin eggs [47,48], it is conceivable that subtle changes introduced in the subplasmalemmal region by these agents might have decoupled the Ca^{2+} -induced Ca^{2+} entry system. In view of the fact that starfish oocytes and eggs are endowed with a fair amount of mRNA encoding molecules homologous to *orai-2* and *STIM1* [49], whether or not SOCE is at work during the late phase of Ca^{2+} increase in the fertilized eggs of sea urchin eggs would be an interesting topic for future study.

Previous work in starfish eggs showed that photoliberation of NAADP induced a Ca^{2+} influx accompanying depolarization of the plasma membrane, which was negated in CaFSW [31,32]. By contrast, in sea urchin eggs, this effect was strongly inhibited by GPN [5], underscoring the role of GPN-sensitive vesicles in shaping CF [50,51]. In starfish eggs, however, 100 μM GPN did not much affect the NAADP-induced membrane depolarization [36]. Thus, species-specific difference may exist on this matter. Furthermore, in view of the finding that opening of the TPCs in sea urchin eggs homogenates may be inhibited by verapamil and diltiazem [52], the suppression of CF by the same drugs (Fig. 1) might be in part due to the inhibition of TPC. However, a study in starfish (*Patiria miniata*) indicated that knockdown of all three TPCs isoforms in the eggs did not suppress the CF, but only altered the timing and pattern of the Ca^{2+} responses at fertilization [53]. Hence, it is not likely that, at least in starfish eggs, the generation of CF is contributed by TPC, which might as well represent a sodium channel [54].

Our observation that disruption or dislocation of vesicles and granules in the egg cortex prior to fertilization consistently suppresses the CF raised the possibility that the integrity of these vesicles beneath the plasma membrane is essential for the production of CF. Obviously, it is not conceivable that these vesicles and granules *per se* are exclusively accountable for the synchronized Ca^{2+} increase over the entire surface of the egg during the CF. As a Ca^{2+} store, however, CG and the acidic vesicles may either release Ca^{2+} that primes Ca^{2+} influx [55], or augment the CF by providing the aforementioned secondary Ca^{2+} increase after the Ca^{2+} influx (Fig. 8 and 9). In either case, the physical contact or vicinity between

the CG and the plasma membrane would be important for the generation of a full-fledged CF.

During sea urchin fertilization, the sperm fusion with the egg elicits the initial inward current and the membrane depolarization [56,57]. In *P. lividus* eggs, the two phases of the membrane potential depolarization (i.e. a small step potential at the beginning and the large and long-lasting fertilization potential at the later stage) precisely mirror the sperm-induced Ca^{2+} signals, i.e. the CF and Ca^{2+} wave, respectively [58,59]. Given that CF is largely dependent upon the membrane potential, our data would not rule out the possibility that the pretreatment of the eggs with GPN and other agents disrupting or dislocating CG and acidic vesicles might have changed the resting potential of the eggs and thereby exhibited compromised CF at fertilization. The resolution of this issue awaits electrophysiological studies in the future.

The common denominator in the eggs pretreated with GPN, procaine, urethane and NH_4Cl is that the microvilli were drastically changed in their number and shape (Fig. 3, 4 and 5). These changes imply that the actin filaments within the microvilli are drastically rearranged, and it may have considerable impacts on the generation of the CF. Firstly, the reduction in the microvilli number will lead to reduced presentation of the Ca^{2+} channels mediating Ca^{2+} influx through the plasma membrane. Secondly, in view of the fact that actin serves as a Ca^{2+} buffer and thereby as a diffusion barrier [60-64], irregularly elongated microvilli are expected to impede Ca^{2+} influx (Table 1). In support of this idea, hyperpolymerization of subplasmalemmal actin cytoskeleton with jasplakinolide significantly repressed the amplitude of the CF in *A. aranciacus* and *P. lividus* eggs at fertilization [65,66]. Furthermore the amplitude of the Ca^{2+} current through the plasma membrane after the uncaging of NAADP in starfish was also inhibited by the actin drugs [35]. Likewise, treatment of *A. aranciacus* eggs with latrunculin-A, which shifts the actin dynamics towards net depolymerization, induces fertilization-like Ca^{2+} waves and CF as well as plasma membrane depolarization [8,64,67].

It is worth mentioning that stratification of the *P. lividus* eggs disclosed the potential existence of a secondary mechanism that augments the CF (Fig. 8 and 9). This delayed Ca^{2+} increase was observable only when the eggs were fertilized after stratification. This short-lived Ca^{2+} increase lagging the CF is discernible only in the cortex of the centrifugal half where YG are concentrated, raising the possibility that these organelles may also contribute to the enhancement of the CF in *P. lividus* eggs. In a sense that this Ca^{2+} puff takes place a few seconds after the

CF, and not before, such a Ca^{2+} increase temporally linked to the CF is considered distinct from the NAADP-induced Ca^{2+} increase that triggers membrane depolarization and Ca^{2+} increase. In this context, our experiments with stratified sea urchin eggs may provide some new insights into the mechanism of Ca^{2+} increase in the fertilized eggs. Contrary to the report that the sperm initiates the Ca^{2+} increase only from the centripetal part of the stratified *Lytechinus pictus* egg where the ER and the nucleus migrate [29], we noted that the initiation of the sperm-induced Ca^{2+} wave does not discriminate between the egg poles in the stratified eggs of *P. lividus* (Fig. 9). This discrepancy could be due to the species difference or to the variation of the experimental conditions; i.e., a longer time of centrifugation (30 min as opposed to 8-15 min) to have elongated cells in our case. However, even in the study of Lee et al 2000 [29], when multiple sperm fertilized the stratified eggs, the Hoechst-stained sperm nuclei were evident also in the centrifugal egg pole.

In summary, we have shown that the integrity and the physical contact of vesicles and CG beneath the plasma membrane are a prerequisite for a normal Ca^{2+} response at the fertilization of sea urchin eggs. Furthermore, the results obtained from the stratified eggs suggest that the reserve YG [29,5] may also serve as functional Ca^{2+} stores substantiating the CF (Fig. 8 and 9). Clarification of the mechanism by which the the YG-derived local Ca^{2+} increase is functionally linked to the Ca^{2+} influx in either chronological order would be important in understanding the physiological significance of these non-ER Ca^{2+} stores in the egg cortex.

Supplementary Material

Supplementary data.

<http://www.ijbs.com/v15p0757s1.pdf>

Acknowledgements

Authors are grateful to M. Cannavacciuolo and G. Zazo (MEDA, SZN) for collecting the animals from the sea and Davide Caramiello (MARE, SZN) for maintenance of the animals. We acknowledge Dr. E. Garante for his insightful comments on the paper, and G. Gragnaniello, F. Iamunno, R. Graziano and G. Lanzotti at the AMOBIO unit (SZN) for preparing the samples for scanning and transmission electron microscopy. F. Vasilev and N. Limatola have been financially supported by SZN post-doctoral fellowship and SZN/Assemble Plus, respectively.

Author contribution

Conceived and designed the experiments: FV,

LS, JTC. Performed the experiments: FV, LS, NL. Analyzed the data: FV, JTC, NL. Contributed reagents and materials: LS. Wrote the paper: FV, JTC, LS.

Competing Interests

The authors have declared that no competing interest exists.

References

- Jaffe LA. Fast block to polyspermy in sea urchin eggs is electrically mediated. *Nature* 1976;261:68-71.
- Shen SS, Buck WR. Sources of calcium in sea urchin eggs during the fertilization response. *Dev Biol* 1993;157(1):157-69.
- Jaffe LA, Gould M. Polyspermy-preventing mechanisms. In *Biology of Fertilization* Metz CB, Monroy A, eds. Academic Press, New York; 1985;223-250.
- Santella L, Limatola N, Chun JT. Actin cytoskeleton and fertilization in starfish eggs. In: Sawada H, et al. eds. *Sexual Reproduction in Animals and Plants*, Springer Verlag, Japan; 2014:147-155.
- Churchill GC, Okada JY, Thomas M, et al. NAADP mobilizes Ca²⁺ from reserve granules, lysosome-related organelles in sea urchin eggs. *Cell*. 2002;111(5):703-8.
- Churchill GC, Galione A. NAADP induces Ca²⁺ oscillations via a two-pool mechanism by priming IP₃- and cADPR-sensitive Ca²⁺ stores. *EMBO J*. 2001;20(11):2666-2671.
- Henson JH, Begg DD. Filamentous actin organization in the unfertilized sea urchin egg cortex. *Dev Biol*. 1988;127(2): 338-348.
- Lim D, Lange K, Santella L. Activation of oocytes by latrunculin A. *FASEB J* 2002;16(9):1050-1056.
- Chun JT, Puppo A, Vasilev F, et al. The biphasic increase of PIP₂ in the fertilized eggs of starfish: new roles in actin polymerization and Ca²⁺ signaling. *PLoS One*. 2010;5:e14100.
- Ohlendieck K, Lennarz WJ. Role of the sea urchin egg receptor for sperm in gamete interactions. *Trends Biochem Sci*. 1995;20(1):29-33.
- Giusti AF, Hoang KM, Foltz KR. Surface localization of the sea urchin egg receptor for sperm. *Dev Biol*. 1997;184(1): 10-24.
- Tilney LJ, Jaffe LA. Actin, microvilli, and the fertilization cone of sea urchin eggs. *J Cell Biol*. 1980;87(3):771-82.
- Carron CP, Longo FJ. Relation of cytoplasmic alkalinization to microvillar elongation and microfilament formation in the sea urchin egg. *Dev Biol*. 1982;89(1):128-137.
- Miyazaki SI, Ohmori H, Sasaki S. Potassium rectifications of the starfish oocyte membrane and their changes during oocyte maturation. *J Physiol*. 1975;246(1):55-78.
- Dale B, de Santis A., Hoshi M. Membrane response to 1-methyladenine requires the presence of the nucleus. *Nature* 1979; 282(5734):89-90.
- Limatola N, Chun JT, Kyozuka K, et al. Novel Ca²⁺ increases in the maturing oocytes of starfish during the germinal vesicle breakdown. *Cell Calcium*. 2015;58(5):500-10.
- Moody WJ, Bosma MM. Hormone-induced loss of surface membrane during maturation of starfish oocytes: differential effects on potassium and calcium channels. *Dev Biol*. 1985;112(2):396-404.
- Dalghi MG, Ferreira-Gomes M, et al. Regulation of the Plasma Membrane Calcium ATPases by the actin cytoskeleton. *Biochem Biophys Res Commun* 2018;506(2):347-354.
- Calaghan SC, Le Guennec JY, White E. Cytoskeletal modulation of electrical and mechanical activity in cardiac myocytes. *Prog Biophys Mol Biol* 2004;84(1):29-59.
- Morgan AJ. Sea urchin eggs in the acid reign. *Cell Calcium*. 2011;50(2):147-56.
- Davis LS, Morgan AJ, Ruas M, et al. Ca²⁺ signaling occurs via second messenger release from intraorganellar synthesis sites. *Curr Biol*. 2008;18(20-24):1612-8.
- Lee HC, Epel D. Changes in intracellular acidic compartments in sea urchin eggs after activation. *Dev Biol*. 1983; 98(2):446-54.
- Ramos IB, Miranda K, Pace DA, et al. Calcium- and polyphosphate-containing acidic granules of sea urchin eggs are similar to acidocalcisomes, but are not the targets for NAADP. *Biochem J*. 2010;429(Pt3):485-495.
- Mallya SK, Partin JS, Valdizan MC, et al. Proteolysis of the major yolk glycoproteins is regulated by acidification of the yolk platelets in sea urchin embryos. *J Cell Biol*. 1992;117(6):1211-21.
- Armant DR, Carson DD, Decker GL, et al. Characterization of yolk platelets isolated from developing embryos of *Arbacia punctulata*. *Dev Biol*. 1986;113(2):342-55.
- Wessel GM, Zaydfudim V, Hsu YJ, Laidlaw M, Brooks JM. Direct molecular interaction of a conserved yolk granule protein in sea urchins. *Dev Growth Differ*. 2000;42(5):507-17.
- Song JL, Wong JL, Wessel GM. Oogenesis: single cell development and differentiation. *Dev Biol*. 2006;300(1):385-405.
- Morgan AJ, Galione A. NAADP induces pH changes in the lumen of acidic Ca²⁺ stores. *Biochem J*. 2007;402(2):301-10.
- Lee HC, Aarhus R. Functional visualization of the separate but interacting calcium stores sensitive to NAADP and cyclic ADP-ribose. *J Cell Sci*. 2000;113(Pt24):4413-20.
- Anderson E. A cytological study of the centrifuged whole, half, and quarter eggs of the sea urchin, *Arbacia punctulata*. *J Cell Biol*. 1970;47(3):711-33.
- Santella L, Kyozuka K, Genazzani AA, et al. Nicotinic acid adenine dinucleotide phosphate-induced Ca²⁺ release. Interactions among distinct Ca²⁺ mobilizing mechanisms in starfish oocytes. *J Biol Chem*. 2000;275(12):8301-6.
- Lim D, Kyozuka K, Gragnaniello G, et al. NAADP+ initiates the Ca²⁺ response during fertilization of starfish oocytes. *FASEB J*. 2001;15(12):2257-67.
- Moccia F, Lim D, Kyozuka K, et al. NAADP triggers the fertilization potential in starfish oocytes. *Cell Calcium* 2004; 36(6):515-24.
- Santella L, Puppo A, Chun JT. The role of the actin cytoskeleton in calcium signaling in starfish oocytes. *Int J Dev Biol*. 2008;52(5-6):571-84.
- Moccia F, Lim D, Nusco GA, et al. NAADP activates a Ca²⁺ current that is dependent on F-actin cytoskeleton. *FASEB J*. 2003;17(13):1907-9.
- Moccia F, Billington RA, Santella L. Pharmacological characterization of NAADP-induced Ca²⁺ signals in starfish oocytes. *Biochem Biophys Res Commun*. 2006;348(2):329-36.
- Galione A, Parrington J, Funnell T. Physiological roles of NAADP-mediated Ca²⁺ signaling. *Sci China Life Sci*. 2011; 54(8):725-32.
- Lee HC, Aarhus R, Gee KR, et al. Caged Nicotinic Acid Adenine Dinucleotide Phosphate. *J Biol Chem*. 1997;272(7): 4172-4178.
- Churchill GC, O'Neill J, Masgrau R, et al. Sperm deliver a new second messenger: NAADP. *Curr Biol*. 2003;13(2):125-128.
- Vasilev F, Chun J, Gragnaniello G, et al. Effects of ionomycin on egg activation and early development in starfish. *PLoS One* 2012;7:e39231.
- Gillot I, Ciapa B, Payan P, et al. The calcium content of cortical granules and the loss of calcium from sea urchin eggs at fertilization. *Dev Biol*. 1991;146(2):396-405.
- Longo FJ, Anderson E. A cytological study of the relation of the cortical reaction to subsequent events of fertilization in urethane-treated eggs of the sea urchin. *Arbacia punctulata*. *J Cell Biol*. 1970;47(3):646-65.
- Vacquier VD, Brandriff B. DNA synthesis in unfertilized sea urchin eggs can be turned on and turned off by the addition and removal of procaine hydrochloride. *Dev Biol*. 1975;47(1):12-31.
- Hylander BL, Summers RG. The effect of local anesthetics and ammonia on cortical granule-plasma membrane attachment in the sea urchin egg. *Dev Biol*. 1981;86(1):1-11.
- Begg DA, Wong GK, Hoyle DHR, et al. Stimulation of cortical actin polymerization in the sea urchin egg cortex by NH₄Cl, procaine and urethane: elevation of cytoplasmic pH is not the common mechanism of action. *Cell Motil Cytoskeleton*. 1996;35(3):210-224.
- Parekh AB, Putney JW Jr. Store-operated calcium channels. *Physiol Rev*. 2005;85(2):757-810.
- Irvine R, Moor RM. Inositol(1,3,4,5)tetrakisphosphate-induced activation of sea urchin eggs requires the presence of inositol trisphosphate. *Biochem Biophys Res Commun*. 1987;146(1):284-290.
- Salido GM, Sage SO, Rosado JA. TRPC channels and store-operated Ca²⁺ entry. *Biochim Biophys Acta - Mol Cell Res*. 2009;1793(2):223-230.
- Musacchia F, Vasilev F, Borra M, et al. De novo assembly of a transcriptome from the eggs and early embryos of *Astropecten aranciacus*. *PLoS One*. 2017;12:e0184090.
- Perez-Terzic CM, Chini EN, Shen SS, et al. Ca²⁺ release triggered by nicotinate adenine dinucleotide phosphate in intact sea urchin eggs. *Biochem J*. 1995;312(Pt3):955-959.
- Galione A, Patel S, Churchill GC. NAADP-induced Ca²⁺ release in sea urchin eggs. *Biol Cell*. 2000;92(3-4):197-204.
- Rahman T, Cai X, Brailoiu GC, et al. Two-pore channels provide insight into the evolution of voltage-gated Ca²⁺ and Na⁺ channels. *Sci Signal*. 2014;7(352):ra109.
- Ramos I, Reich A, Wessel GM. Two-pore channels function in calcium regulation in sea star oocytes and embryo. *Development*. 2014;141(23):4598-609.
- Wang X, Zhang X, Dong XP, et al. TPC proteins are phosphoinositide-activated sodium-selective ion channels in endosomes and lysosomes. *Cell*. 2012;151(2):372-83.

- [55] Moccia F, Nusco GA, Lim D, Kyozyuka K, Santella L. NAADP and InsP3 play distinct roles at fertilization in starfish oocytes. *Dev Biol.* 2006;294(1):24-38.
- [56] McCulloh DH, Chamber EL. Fusion of membranes during fertilization. Increases of the sea urchin egg's membrane capacitance and membrane conductance at the site of contact with the sperm. *J Gen Physiol.* 1992;99(2):137-175.
- [57] McCulloh DH, Ivonnet PI, Landowne D, et al. Calcium influx mediates the voltage-dependence of sperm entry into sea urchin eggs. *Dev Biol.* 2000;223(2):449-62.
- [58] Dale B, De Felice LJ, Taglietti V. Membrane noise and conductance increase during single spermatozoon-egg interactions. *Nature.* 1978;275:217-9.
- [59] Santella L, Limatola N, Chun JT. Calcium and actin in the saga of awakening oocytes. *Biochem Biophys Res Commun.* 2015;460(1):104-113.
- [60] Lange K. Microvillar Ca⁺⁺ signaling: a new view of an old problem. *J Cell Physiol.* 1999;180(1):19-34.
- [61] Lange K. Fundamental role of microvilli in the main functions of differentiated cells: Outline of a universal regulating and signaling system at the cell periphery. *J Cell Physiol.* 2011;226(4):896-927.
- [62] Chun JT, Santella L. Roles of the actin-binding proteins in intracellular Ca²⁺ signaling. *Acta Physiologica* 2009;195(1):61-70.
- [63] Chun JT, Santella L. The actin cytoskeleton in meiotic maturation and fertilization of starfish eggs. *Biochem Biophys Res Commun.* 2009;384(2):141-3.
- [64] Vasilev F, Limatola N, Park DR, et al. Disassembly of subplasmalemmal actin filaments induces cytosolic Ca²⁺ increases in *Astropecten aranciacus* eggs. *Cell Physiol Biochem.* 2018;48(5):2011-2034.
- [65] Puppo A, Chun JT, Gagnaniello G, et al. Alteration of the cortical actin cytoskeleton deregulates Ca²⁺ signaling, monospermic fertilization, and sperm entry. *PLoS One* 2008;3(10):e3588.
- [66] Chun JT, Limatola N, Vasilev F, et al. Early events of fertilization in sea urchin eggs are sensitive to actin-binding organic molecules. *Biochem Biophys Res Commun.* 2014;450(3):1166-1174.
- [67] Moccia F. Latrunculin A depolarizes starfish oocytes. *Comp Biochem Physiol A Mol Integr Physiol.* 2007;148(4):845-52.